

# ENERGY TRANSFER IN A VORTEX INDUCED VIBRATING TETHERED CYLINDER SYSTEM

K. Ryan, M.C. Thompson, K. Hourigan  
 Fluids Laboratory for Aeronautical and Industrial Research (FLAIR)  
 Department of Mechanical Engineering  
 Monash University, Clayton VIC Australia

## ABSTRACT

Flow induced vibration of a tethered body submerged within a uniform flow represents a fundamental example of fluid-structure interaction. However, little research in this field has been undertaken. This paper presents results from a direct numerical simulation of the flow past a tethered cylinder with mass ratio less than 1. The Navier-Stokes and dynamic equations of motion of the cylinder are solved using a Galerkin spectral element/Fourier method. The fluid forces acting on the cylinder, as well as the tension in the tether are computed and used to determine the resulting cylinder motion. The energy transfer from the fluid to the cylinder is calculated, and two distinct modes of oscillation are observed.

## INTRODUCTION

A simple extension to the problem of a hydro-elastically mounted oscillating cylinder is a cylinder whose motion is confined to an arc by a restraining tether. By considering a wide range of mass ratios,  $m^*$  (the mass of the cylinder divided by the mass of the displaced fluid), we may allow for both buoyant bodies ( $m^* < 1$ ) and dense bodies ( $m^* > 1$ ), and hence describe a parameter space encompassing a range of practical applications. To date, little progress has been made regarding the fluid-structure interaction of a tethered body, and virtually no work has been published regarding the flow around a tethered cylinder. In this paper, we report on the development of a new numerical code used to simulate the two-dimensional flow field around a tethered cylinder. This code has been validated against preliminary experiments performed in the Monash FLAIR water channel.

Most previous work regarding tethered bodies has focused on the free surface interaction with tethered buoys (Shigai *et al.* (1969), and Ogihara (1988)). In each of these studies, the tethered bodies oscillate due to the combined effect of a uniform (or sheared) free stream and free surface waves. This combination induces complicated body motion, which inhibits clear interpretation of the individual forcing mechanisms acting on the body. Only the related studies of Williamson *et al.* (1997), Govardhan *et al.* (1997), and Jauvtis *et al.* (2001) deal purely with the interaction of a uniform flow field and a tethered body (specifically a tethered sphere). Their experimental study was performed by placing spheres of various mass ratios and tether lengths into a water channel at various flow speeds. Sustained, large peak-to-peak oscillations in the transverse flow-field direction were noted, with amplitudes in the order of two sphere diameters. Small stream-wise oscillations of the order of about 0.4 sphere diameters were also observed. Their results were independent of sphere mass ratio or tether length if they were plotted against the reduced velocity ( $U^* = U/f_n D$ , where  $f_n$

is the natural frequency of the tethered sphere system). From this information, four distinct modes of shedding were observed corresponding to local maxima in the peak-to-peak transverse oscillation of the sphere (see figure 4b in Govardhan *et al.* (1997)). Two of the observed modes were present for low reduced velocity experiments ( $U^* < 25$  corresponding to  $m^* < 1$ ). It may be anticipated that the flow around a circular cylinder will follow similar phenomenon.

This investigation presents a new numerical algorithm for simulating the flow past a two-dimensional tethered body, and relates the solutions obtained to the vortex-induced oscillation of bluff bodies. A cylinder mass ratio,  $m^* = 0.833$  was simulated. It was found that the oscillation frequency remains close to the vortex shedding frequency of the flow as in Angrilli *et al.* (1974) and Govardhan *et al.* (2000). The energy input from the fluid to the cylinder over one oscillation cycle was calculated and used to establish two separate modes of vortex induced oscillation.

## PROBLEM FORMULATION

The coordinate system and geometry of the problem are shown in Figure 1. The fluid forces acting on the tethered body are composed of Drag ( $F_D$ ), Lift ( $F_L$ ), and Buoyancy ( $B$ ) terms. A restoring tension force ( $T$ ) in the tether is also present.

The problem is fully described in two dimensions by the coupled system of the incompressible Navier-Stokes equations (equation 1a and 1b) and the equations of motion describing the body acceleration in response to calculated fluid forces (equations 2a and 2b).

$$\frac{\partial \mathbf{u}'}{\partial t} + (\mathbf{u}' \cdot \nabla') \mathbf{u}' = -\frac{1}{\rho_f} \nabla' p' + \frac{1}{Re} \nabla'^2 \mathbf{u}' \quad (1a)$$

$$\nabla' \cdot \mathbf{u}' = 0, \quad (1b)$$

where  $\mathbf{u}'$  is the velocity field and  $p'$  is the pressure field.

$$\ddot{x} = \frac{\gamma}{L^2 M^*} \left[ (L^2 - x^2) C_D - x \left\{ y \left( C_L + \frac{\pi}{2} (1 - M^*) \frac{1}{Fr^2} \right) \right\} \right] \quad (2a)$$

$$\ddot{y} = \frac{\gamma}{L^2 M^*} \left[ (L^2 - y^2) \left( C_L + \frac{\pi}{2} (1 - M^*) \frac{1}{Fr^2} \right) - yx C_D \right] \quad (2b)$$

where  $Fr$  is the Froude number and  $\gamma = \frac{2 U^2}{\pi D}$ . Note that  $\gamma$  is dimensional and has units of acceleration.

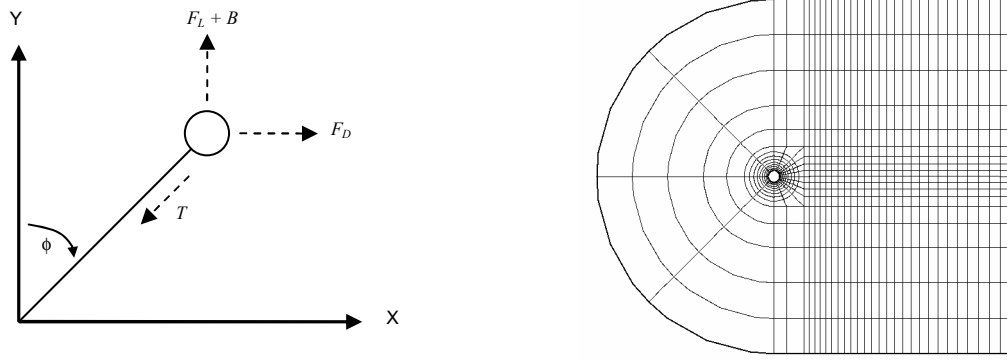


**Figure 1** (Left) Schematic of tethered cylinder system. (Right) Two-dimensional macro element mesh used in the numerical simulations.

## NUMERICAL METHOD

A Galerkin spectral element method was used to simulate the flow field. An inertial reference frame attached to the cylinder is employed such that a moving mesh implementation is not required. This simplifies the numerical process, and allows for a detailed domain resolution analysis to be performed. Details of the numerical coupling between the fluid solver and the body equations of motion may be found in Pregalato, *et al.* (2002).

A comprehensive resolution study was performed for a stationary cylinder at a Reynolds number,  $Re = 500$  (based on cylinder diameter), and also for a tethered (moving) cylinder at a Reynolds number,  $Re = 200$ . For each study, the order of the interpolating polynomials was increased from  $N = 5$  to  $N = 9$  to test for grid resolution. The variation in shedding frequency, lift and drag between the values at  $N = 7$  and  $N = 9$  are less than 1%. Furthermore, for the fixed cylinder, the values of all measures for  $N = 8$  (used in all simulations) compare to within 1% of the numerical values of Blackburn, *et al.* (1999) and Henderson (1995). The macro-element mesh used for the investigation is shown in figure 1 (right).

## RESULTS

The problem is essentially that of a pendulum with external forcing applied, hence, the natural frequency ( $f_n$ ) is given by

$$f_n = \frac{1}{2\pi} \sqrt{\frac{T}{ML}} \quad (3)$$

In a similar fashion as the Strouhal number is used as a non-dimensional frequency parameter for the wake flow field of stationary body, the natural frequency of the system may be rewritten in a non-dimensional form as,

$$S_n = \frac{f_n D}{U} = \frac{1}{U^*} \quad (4)$$

By applying a force balance to the tethered system (see figure 1), the tension force term ( $T$  in equation 3) may be rewritten in terms of the Drag coefficient, Lift coefficient and Froude number:

$$S_n = \left( \frac{1}{\sqrt{2\pi^3}} \right) \sqrt{\frac{C_D \cos \phi + \frac{\pi}{2} \left( \frac{C_L + (1-M^*)}{Fr^2} \right) \sin \phi}{M^* L^*}} \quad (5)$$

As in the work of Williamson *et al.* (1997), the reduced velocity is taken as the controlling parameter. The reduced velocity may be altered independently of the Reynolds number by altering the Froude number term in equation 5, essentially changing the gravity term. The Reynolds number was held fixed at  $Re = 200$  for all simulations. This value was chosen in order to simulate as closely as possible a range of experimental conditions, as both the drag coefficient and vortex shedding frequency may be considered essentially constant for the range  $200 < Re < 10^5$ . A fixed tether length of  $L^* = 5.5$  and mass ratio of  $m^* = 0.833$  were chosen for the investigation. These particular values were chosen to provide direct comparisons with preliminary experiments being conducted simultaneously in the Monash FLAIR water channel.

The cylinder motion may be represented by the addition of a mean layover angle component ( $\phi_{mean}$ ) and a time dependent component ( $\phi$ ). By considering the mean drag, mean lift ( $C_{L(mean)} = 0$ ), and buoyancy, an estimate may be made of the mean layover angle as a function of reduced velocity. This is given by:

$$\tan(\phi_{mean}) = \left( \frac{2}{\pi} \right) \left( \frac{C_D Fr^2}{(1-M^*)} \right) \quad (6)$$

A predicted mean layover angle (using equation 6) is plotted in Figure 2 (left) as a function of reduced velocity. The value of  $C_D$  was obtained from the drag coefficient data for a stationary cylinder at the corresponding Reynolds number of  $Re = 200$  (Drag coefficient taken from Henderson (1995)). Also shown is the actual mean angle,  $\phi$ , obtained through the numerical simulations. Preliminary data from the water channel experiments are also presented. Both the

simulated and experimental results follow the predicted response closely for low reduced velocities. At higher layover angles ( $\phi > 50$  degrees) the numerical results begin to deviate from the prediction curve. At these high layover angles, the drag for the tethered cylinder increases slightly when compared to that of the stationary cylinder. This phenomenon is similar to that observed by Blackburn *et al.* (1999) in their oscillating cylinder experiments. The mean drag is presented in Figure 2 (right). A small peak at a reduced velocity,  $u^* = 2.5$  is noticeable, coinciding with a peak in in-line cylinder oscillations. No noticeable deviation is observed in the mean tether angle coinciding with this peak in the drag force as, at these low reduced velocities, the tether angle is dominated by buoyancy forces. A significant decrease in the mean drag is observed at higher reduced velocities, coinciding with a reduction in the rate of increase of the mean layover angle.

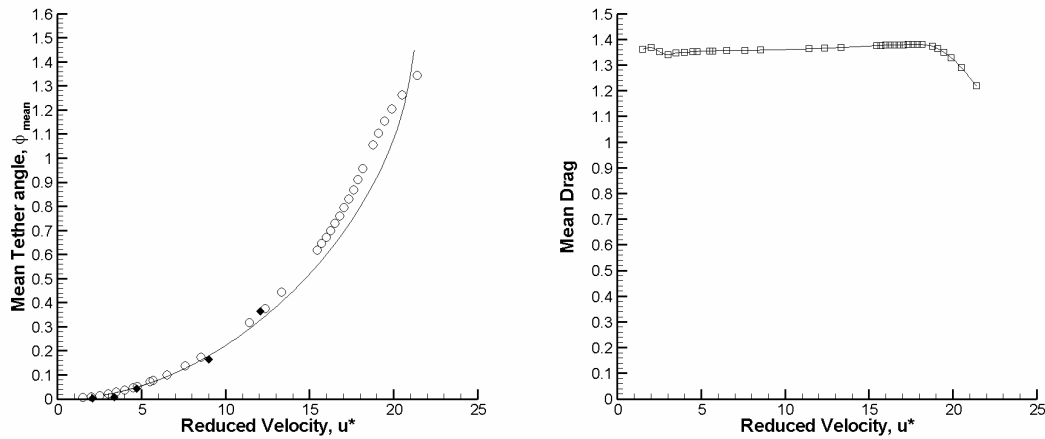


**Figure 2.** (Left) Mean angle of tether (in degrees) as a function of reduced velocity: solid line denotes predicted response; O, numerical results;  $\blacklozenge$ , experimental results. (Right) Mean Drag coefficient as a function of reduced velocity.

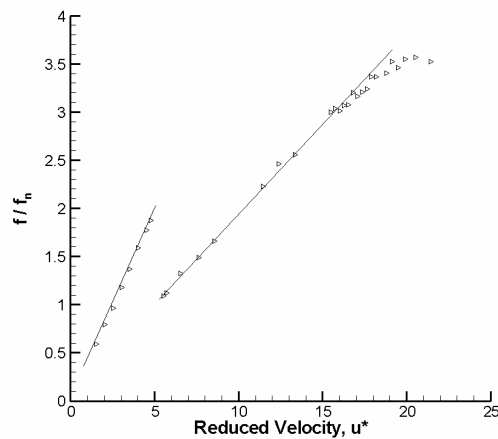


**Figure 3.** Oscillation frequency ratio,  $f/f_n$  as a function of reduced velocity, Solid line represents the fixed cylinder shedding frequency.

The cylinder oscillation frequency, normalized against the shedding frequency, is presented in figure 3 as a function of reduced velocity. Also shown is the vortex shedding frequency for a stationary cylinder (solid line). It appears that the oscillations are due to a resonance between the oscillation frequency of the tethered body and the wake vortex shedding frequency. At low  $u^*$ , the oscillations are essentially inline and the cylinder oscillates with the drag frequency (at twice the Strouhal number), however, at higher  $u^*$ , the cylinder oscillates with the lift frequency. The coincidence between the cylinder oscillation and the shedding frequency is in agreement with the results of Angrilli, *et al.* (1974) and Govardhan, *et al.* (2000). At higher reduced velocities, the normalized oscillation frequency departs significantly from the vortex shedding frequency for a stationary cylinder. At these high reduced velocities, the cylinder essentially oscillates transverse to the flow field. For a hydro-elastically mounted cylinder in equivalent conditions, it would be anticipated that the cylinder would oscillate in the lower mode of shedding, with the oscillation frequency becoming desynchronized at high reduced velocities (Govardhan, *et al.* (2000)). This phenomenon would account for the de-synchronization observed in figure 3 at  $u^* > 20$ .

The energy input from the fluid to the cylinder and RMS  $\phi'$  are presented in Figure 4 (left). Two distinct peaks are observed in the RMS  $\phi'$  plot. The first, at  $u^* = 2.5$ , represents a peak in the cylinder oscillations in a direction inline with the flow field. This peak in the inline oscillation is due to a resonance between the natural frequency of the tethered cylinder system and the drag frequency and agrees favorably with theory presented in Blevins(1990). The second peak occurs at  $u^* = 20$  and represents a peak in the cylinder oscillations transverse to the flow field. Two peaks are also observed in the energy input; however the peak for the inline oscillations is very small in magnitude. The reduction in energy and RMS  $\phi'$  for  $u^* > 20$  is once again in agreement with the findings of Govardhan, *et al.* (2000),

and represents the case of a hydro-elastically mounted cylinder oscillating in the lower mode. The drag, lift and in-line RMS force values are presented in figure 4 (right) where the 'in-line' force is defined as force acting in the direction of the cylinder motion and is essentially a vector addition of both the lift and drag forcing terms. Both the drag and in-line RMS forces show a distinct peak at a reduced velocity of 2.5, where the cylinder resonates with the drag frequency. A further peak in the RMS drag force occurs at a reduced velocity of 17.5, however the inline RMS force peaks at a reduced velocity of 20 as the lift force component dominates the drag force at these high mean layover angles. Beyond a reduced velocity of 20, the lift, drag and in-line forces reduce markedly in agreement with the findings of Govardhan, *et al.* (2000).

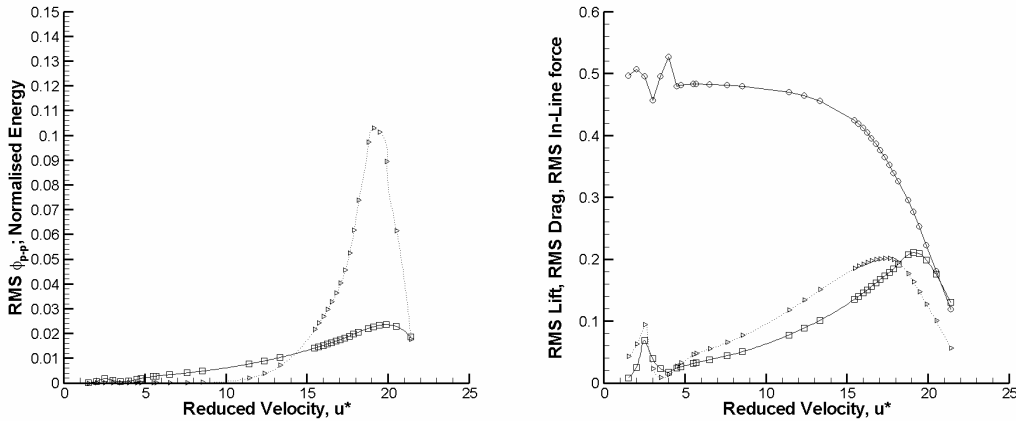


**Figure 4.** (left),  $\square$ ,  $\text{RMS } \phi'$ ,  $\triangleright$ , Normalised Energy input as a function of reduced velocity. (right),  $\circ$ , RMS Lift,  $\triangleright$ , RMS Drag and,  $\square$ , RMS 'in-line' force as a function of reduced velocity.

## CONCLUSION

A Galerkin spectral element numerical algorithm has been used to simulate the flow past a two-dimensional tethered body. A low mass ratio tethered cylinder was studied, and two modes of shedding were established and may be broadly described as an in-line and transverse oscillation respectively. Both oscillations appear to occur in agreement with previous studies of hydro-elastically mounted cylinders.

## ACKNOWLEDGMENTS

We gratefully acknowledge the supported by the Australian Research Council, the Victorian Partnership for Advanced Computing (VPAC) and the Australian Partnership for Advanced Computing (APAC).

## REFERENCES

- ANGRILLI, F., DI SILVO, G. AND ZANARDO, A. 1974 HYDRO-ELASTICITY STUDY OF A CIRCULAR CYLINDER IN A WATER STREAM, *FLOW-INDUCED STRUCTURAL VIBRATIONS*, NAUDASCHER (ED.), SPRINGER, BERLIN
- BLACKBURN, H. M. AND HENDERSON, R. D. 1999 A STUDY OF TWO-DIMENSIONAL FLOW PAST AN OSCILLATING CYLINDER. *JOURNAL OF FLUID MECHANICS*. 385, 255-286
- BLEVINS, B. D. 1990 *FLOW-INDUCED VIBRATIONS*. VAN NOSTRAND REINHOLD.
- GOVARDHAN, R. AND WILLIAMSON, C. H. K. 1997 VORTEX-INDUCED MOTIONS OF A TETHERED SPHERE. *JOURNAL OF WIND ENGINEERING*. 69-71, 375-385
- GOVARDHAN, R. AND WILLIAMSON, C. H. K. 2000 MODES OF VORTEX FORMATION AND FREQUENCY RESPONSE OF A FREELY VIBRATING CYLINDER. *JOURNAL OF FLUID MECHANICS*. 420, 85-130
- HENDERSON, R. D. 1995 DETAILS OF THE DRAG CURVE NEAR THE ONSET OF VORTEX SHEDDING. *PHYSICS OF FLUIDS*. 7, 2102-2104
- JAUVTIS, N., GOVARDHAN, R. AND WILLIAMSON, C. H. K. 2001 MULTIPLE MODES OF VORTEX-INDUCED VIBRATION OF A SPHERE. *JOURNAL OF FLUIDS AND STRUCTURES*. 15, 555-563
- OGIHARA, K. 1988 THEORETICAL ANALYSIS ON THE TRANSVERSE MOTION OF A BUOY BY A SURFACE WAVE. *APPLIED OCEAN RESEARCH*. 2, 51-56
- SHI-IGAI, H. AND KONO, T. 1969 STUDY ON VIBRATION OF SUBMERGED SPHERES CAUSED BY SURFACE WAVES. *COASTAL ENGINEERING JAPAN*. 12, 29-40
- WILLIAMSON, C. H. K. AND GOVARDHAN, R. 1997 DYNAMICS AND FORCING OF A TETHERED SPHERE IN A FLUID FLOW. *JOURNAL OF FLUIDS AND STRUCTURES*. 11, 293-305